11th Australasian Fluid Mechanics Conference
University of Tasmania, Hobart, Australia
14-18 December 1992

LARGE AMPLITUDE MODE 2 DEEP-WATER INTERNAL SOLITARY WAVES

Andrew STAMP and Ross W. GRIFFITHS

Research School of Earth Sciences
Australian National University
GPO Box 4, Canberra, ACT 2601, AUSTRALIA

ABSTRACT

Accurate experimental measurements of deep-water internal solitary waves are compared to weakly nonlinear theory and fully nonlinear numerical solutions. At large amplitudes such waves contain a region of fluid trapped within closed streamlines and hence may transport mass over large distances. The speed of these waves increases linearly with increasing amplitude over the entire range of small and large amplitudes. In contrast to small-amplitude waves with open streamlines, the wavelength of large-amplitude waves increases linearly with increasing amplitude, so that the wave shape remains constant. The behaviour of these large-amplitude waves during reflection from a solid vertical boundary is dependent on amplitude and the wave always suffers a negative spatial phase shift. The head-on collision of two waves of equal amplitude is similar to a reflection.

INTRODUCTION

The propagation of solitary waves in fluids has been of interest since Scott-Russell (1837, 1844) first observed a surface water wave of finite amplitude and permanent form. The permanent form is due to a balance between dispersion and nonlinearity. Recent interest has centred on internal solitary waves in density stratified fluids. These waves are important in both atmospheric physics and oceanography, with the Morning Glory phenomenon in northern Australia (Christie et al., 1978) and, possibly, Jupiter's Great Red Spot (Maxworthy and Redekopp, 1976) being stunning examples.

This study considers deep-water waves; these waves have wavelengths much smaller than the total fluid depth but much greater than the depth of the stratification. At small amplitudes such waves have open streamlines and are accurately described by the weakly nonlinear theory of Benjamin (1967) and Davis and Acrivos (1967). However at large amplitudes they contain fluid trapped within closed streamlines, implying that these waves may transport mass over large distances, and the fully nonlinear theory of Tung et al. (1982) is required.

DESCRIPTION OF EXPERIMENTS

All of the experiments were carried out in a glass tank 180 cm long, 30 cm deep and 15 cm wide. A stratified fluid was created by carefully floating fresh water on top of a layer of saline water through two diffusers and allowing the interface to thicken by diffusion. The ratio of layer depth H to interface thickness h was very large. To visualise the waves, surfaces of constant density within the fluid were marked using dyed water-insoluble droplets. In selected experiments the centre of the interface was also marked with droplets or water soluble food dye. Waves were generated by a paddle (of depth 7 cm extending across the entire tank width and centred on the middle of the interface) which was pushed a distance of 25 cm to a point at which it fitted between two polystyrene baffles.

There are two independent parameters governing the propagation of internal waves: the density differences associated with the stratification and the wave amplitude. The density difference was obtained by measuring the density of samples taken from the upper and lower fluid layers. Measurements of the amplitude, wavelength and time of arrival were made every 5 cm along the tank. The amplitude is defined as the maximum displacement of any streamline. Hence the nondimensional amplitude ε is given by the maximum value of the nondimensional perturbation streamfunction

$$\varepsilon = \max\left(\frac{\psi - z}{h}\right) \approx \frac{\psi(\pm h) - h}{h} \quad . \qquad (1)$$

The wavelength ℓ is defined, in accordance with the weakly nonlinear theory of Benjamin (1967), as the half width at the height where the amplitude is half its maximum value. The dimensionless amplitude is then $\tilde{\ell} = \ell/h$.

Three sets of experiments were conducted. The first set of experiments investigated the profile, speed and attenuation of a single wave. The second set investigated the behaviour of waves during reflection from a solid vertical boundary (the tank end walls), and the final set of experiments investigated the head-on collision of two waves. In each experiment the upper layer density was 1.00 g cm^3. For the first set lower layer densities from 1.05 to 1.20 were used, whereas in all of the reflection and collision experiments the lower layer density was ρ_L = 1.10 g cm^3. Different amplitudes were obtained by allowing the waves to propagate different distances from the wave-maker before colliding.

RESULTS

Observations

The paddle generation technique was able to generate a single large-amplitude wave as little as 10 cm from the point at which the paddle stopped. Once the paddle stopped the displaced interfacial fluid trapped against the paddle collapsed along the interface and became unstable to backward breaking billows. Instability caused some of the fluid displaced by the paddle to be ejected backwards, causing the intrusion to have a distinct lengthscale. Consequently the intrusion had to propagate only a small distance before it formed a wave. The initial amplitude was always $\varepsilon \approx 2.9$. Thus we postulate that wave breaking occurred because waves of greater amplitudes were unstable in the experimental stratification.

The principal difference between large- and small-amplitude waves is the presence of the closed streamline region in large-amplitude waves. We visualized the motion associated with the closed streamline region using droplets and food dye made neutrally buoyant at the centre of the interface. In some experiments the closed streamline region consisted of two counter rotating cells similar to those

observed experimentally by Maxworthy (1980) and numerically by Tung et al. (1982). In other experiments the two cells either did not rotate or were not observed at all. However it is believed that these counter rotating cells were always present and were in some cases not visible (although the nondimensional amplitudes were large) because the physical dimensions of the waves were small.

Some of the fluid entrained into the closed streamline region during generation remained trapped for the lifetime of the region. On the other hand, fluid from within the closed streamline region was continually ejected behind the wave, resulting in an increased interface thickness behind the wave. It was also noted that dye was ejected along the central horizontal axis of the wave from the rear of the closed streamline region in a laminar manner, whereas the immiscible marker droplets were ejected from the upper and lower portions of the rear of the closed streamline region in a turbulent manner. Offsetting this mass loss is a continual entrainment of fluid into the recirculating region from ahead of the wave. Dye initially in the interface is mixed slowly into the recirculating region, at a constant rate along the entire length of the streamlines bounding this region, by turbulent diffusion.

Plan view observations indicated that the waves were two dimensional. The wave front was always straight and perpendicular to both sidewalls and neither dye nor droplets within the closed streamline region moved along the axis of the wave front; indicating that velocities in this direction were small.

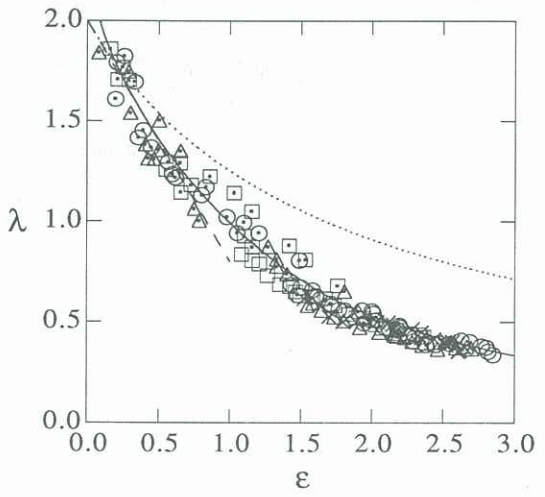

Fig.1. The wave speed parameter $\lambda = \sigma g h/c^2$ and dimensionless wave amplitude plotted against each other for four experiments with lower layer densities: $\rho_L = 1.05$ △, $\rho_L = 1.10$ □, $\rho_L = 1.15$ ○ and $\rho_L = 1.20$ g cm^{-3} ×. The Davis and Acrivos (1967) experimental data $\rho_L = 1.052$ △, $\rho_L = 1.095$ ▪ and $\rho_L = 1.168$ ⊙ are plotted to extend the range of wave amplitudes. The weakly nonlinear theories of Benjamin (1967) (. . . . .) and Davis and Acrivos (1967) (– – –) and the fully nonlinear numerical solution of Tung et al. (1982) (———) for H/h=40 are plotted.

Wave Speed

The principal quantity of interest in theoretical investigations of internal solitary waves is the wave speed c, which is a function of amplitude. Our measurements are shown on Fig.1, where the weakly nonlinear theory of Benjamin (1967), the experimental results and weakly nonlinear theory of Davis and Acrivos (1967) and the fully nonlinear numerical solution of Tung et al. (1982) for H/h=40 are plotted for comparison. Our results and those of Davis and Acrivos (1967) are accurately represented by

$$\frac{c}{c_o} = 1 + 0.4930\,\varepsilon \qquad (2)$$

over the range $0.08 \le \varepsilon \le 2.85$, where c_o is the speed of long linear waves. Several conclusions follow: first, since all the data collapsed onto a single curve over the entire range of amplitudes, the dependence of the wave speed on the density difference was limited to $c_o \propto \sqrt{\sigma}$, as for long linear waves. Second, despite the qualitative differences between the small- and large- amplitude waves, the wave speed increased linearly with increasing amplitude over the entire range of amplitudes. This is in contrary to the conclusion of Davis and Acrivos (1967) that at small amplitudes the wave speed increases linearly with increasing amplitude while at large amplitudes the wave speed increases at a significantly slower rate. The present results are in agreement with the fully nonlinear numerical solution (using the Boussinesq approximation) of Tung et al. (1982) for H/h = 40.

Aspect Ratio

Wavelength-amplitude scaling is fundamental in the theoretical analysis of solitary waves. Fig.2 shows the wavelength and amplitude plotted against each other. The wavelength increased linearly with increasing amplitude and hence the wave aspect ratio remained constant; at $\ell/\varepsilon \approx 2.2$ here. This result is in stark contrast to the prediction of weakly nonlinear theory that, in order to maintain a permanent form, the wavelength must be smaller for larger amplitudes. The reason for this difference is the presence of a region of closed streamlines in the large-amplitude waves.

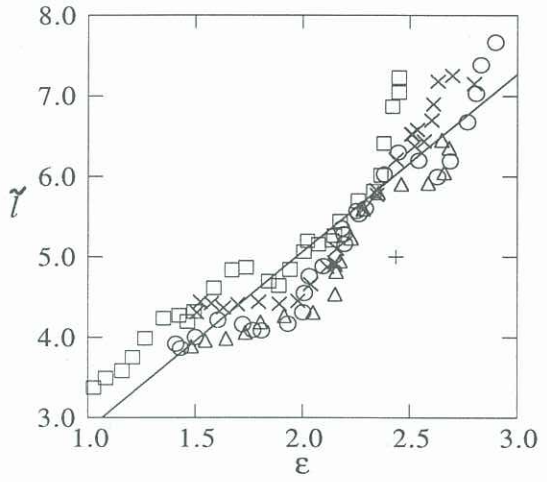

Fig.2. The wavelength and amplitude plotted against each other for the four experiments of Fig.1. The point + is from the fully nonlinear numerical solution of Tung et al. (1982) for H/h=40.

Amplitude Attenuation

An obvious difference between the small- and large-amplitude waves was the rate of amplitude attenuation. The large-amplitude waves suffered such rapid attenuation that they were able to complete only one transit of the tank before decaying into small-amplitude waves. In contrast, the small-amplitude waves propagated with only gradual attenuation and completed many transits of the tank. Fig.3 shows the amplitude plotted against wave displacement.

The amplitude decreased linearly with displacement and the attenuation rate decreased with increasing density difference. It was not possible to determine whether attenuation occurred predominantly due to viscous wall effects or wave breaking (the ejection of fluid from within the closed streamline region). However, the Reynolds number for the flow over the wave was larger for larger density differences.

Reflections

The behaviour of small- and large-amplitude waves was qualitatively different during reflections. The behaviour of

small-amplitude waves was independent of the amplitude of the incident wave and there was no apparent energy loss; the reflected wave was always identical to the incident wave. Conversely, the behaviour of large-amplitude waves was dependent on amplitude and the reflected wave was always smaller than the incident wave. However, for both small- and large-amplitude waves the maximum amplitude of the distorted wave was double the amplitude of the incident wave.

Of the large-amplitude waves the smaller ones collapsed away from the boundary without breaking but the fluid trapped within the incident wave was ejected behind the reflected wave. As a consequence, these waves suffered a large decrease in amplitude and propagated away from the reflecting wall as a small-amplitude wave. The largest waves broke backwards, in a manner similar to that during wave generation. Associated with the wave breaking was the ejection of some trapped fluid and a subsequent large decrease in amplitude. Waves of intermediate amplitude did not break or eject large amounts of fluid and experienced the smallest decrease in amplitude.

Head-on Collisions

The investigation of the head-on collision of two waves of equal amplitude was restricted to incident waves of very large amplitudes ($\varepsilon \approx 2.3$). The behaviour was similar to the reflection of a wave of the same amplitude from a solid vertical boundary: the fluid trapped within each wave reversed direction and was transported away from the collision along the path by which it approached. As when reflecting from a wall, the waves broke as they collapsed away from each other. During this process a small amount of fluid was ejected by each wave, thus decreasing the amplitude of the reflected waves and thickening the interface between the two waves. This thickened section of interface subsequently collapsed forming secondary, smaller waves.

When two waves of different amplitude collided, the behaviour is similar to that for two waves of equal amplitude, but with an exchange of fluid from the larger incident wave to the smaller incident wave. This transfer of fluid is required in order to satisfy conservation of momentum. Despite that fact that most of the trapped fluid is reflected during collision, these waves are essentially solitons as the two waves pass through each other unchanged by the collision.

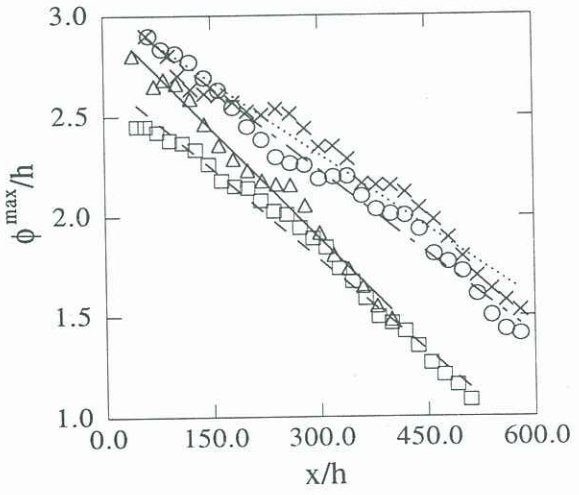

Fig.3. The amplitude plotted against wave displacement for the four experiments of Fig.1.

CONCLUSIONS

Our experiments with individual interfacial solitary waves show that at large amplitude they carry mass over large distances. The fluid being transported is, however, continually exchanged through addition from ahead of the wave and ejection at the rear, so that passive tracer is transported only a finite distance. The wave speed varies linearly with dimensionless amplitude, a result which is in accord with previous numerical solutions but contrary to predictions of weakly non-linear theory. Along with the presence of a region of closed streamlines within very large-amplitude waves, we find that their aspect ratio is independent of amplitude. These waves pass through each other unchanged and in this way behave as solitons. However, they also behave as "particles" in the sense that most of the fluid carried within the recirculating region is reflected in a head-on collision.

REFERENCES

BENJAMIN, T B (1967) Internal waves of permanent form in fluids of great depth. J Fluid Mech, 29, 559.

CHRISTIE, D K, MUIRHEAD, K J and HALES, A L (1978) On solitary waves in the atmosphere. J Atmos Sci., 35, 805.

DAVIS, R E and ACRIVOS, A (1967) Solitary internal waves in deep-water. J Fluid Mech, 29, 593.

MAXWORTHY, T (1980) On the formation of nonlinear internal waves from the gravitational collapse of mixed regions in two and three dimensions. J Fluid Mech, 96, 47.

MAXWORTHY, T and REDEKOPP, L G (1976) A solitary wave theory of the Great Red Spot and other observed features in the Jovian atmosphere. Icarus 29, 261.

SCOTT-RUSSELL, J (1837) Report on waves. Brit Assoc Adv Sci No. 417.

SCOTT-RUSSELL, J (1844) Report on waves. Brit Assoc Adv Sci No.311.

TUNG, K, CHAN, T F and Kubota, T (1982) Large amplitude internal wave of permanent form. Stud Appl Math, 66, 1.